SAND75-0655
Unlimited Release

BREMSSTRAHLUNG CONVERTORS: MATERIALS DESIGN AND DEVELOPMENT

Ronald E. Allred

Prepared by Sandia Laboratories, Albuquerque, New Mexico 87115 and Livermore, California 94550 for the United States Atomic Energy Commission under Contract AT (29-1)-789

March 1976

Sandia Laboratories

SF 2900 Q(7-73)

When printing a copy of any digitized SAND Report, you are required to update the markings to current standards.

Issued by Sandia Laboratories, operated for the United States Energy Research and Development Administration by Sandia Corporation.

NOTICE

This report was prepared as an account of work sponsored by the United States Government. Neither the United States nor the United States Energy Research and Development Administration, nor any of their employees, nor any of their contractors, subcontractors, or their employees, makes any warranty, express or implied, or assumes any legal liability or responsibility for the accuracy, completeness or usefulness of any information, apparatus, product or process disclosed, or represents that its use would not infringe privately owned rights.

Printed in the United States of America

Available from
National Technical Information Service
U. S. Department of Commerce
5285 Port Royal Road
Springfield, VA 22151
Price: Printed Copy $4.50 Microfiche $2.25

SAND75-0655

Bremsstrahlung Convertors: Materials Design and Development*

R. E. Allred
Sandia Laboratories, Albuquerque, New Mexico 87115

ABSTRACT

An improved bremsstrahlung convertor for use at high electron beam energies has been developed. The convertor consists of three main components: (1) conversion foil, (2) electron scavenger and (3) impulse shield. Structural failures of the impulse shield were experimentally determined to be caused by shock wave interactions. Convertor materials and design modifications were aimed at attenuation of the magnitude of the shock and maximization of energy absorption by the convertor materials. Techniques proven successful included the introduction of porosity into electron scavenger and impulse shield materials, the use of a standoff between the conversion foil and the electron scavenger, the insertion of a gap between the scavenger and impulse shield, and the use of advanced composite materials for the impulse shield. These modifications have increased the convertor operating range from 4 cal/gm Au to over 8 cal/gm Au. Kevlar 49 reinforced-resin composites have proven to have the best combination of strength, stiffness, toughness and x-ray transport properties for use as bremsstrahlung convertor impulse shields.

*This work was supported by the United States Energy Research & Development Administration.

Introduction

The bremsstrahlung reaction in which an accelerated electron is scattered and radiates is well known.[1] Bremsstrahlung sources based upon this principle are used for a wide variety of photon effects experiments on electronic circuits and materials. These sources are generally driven by a high energy pulsed electron beam generator. The energetic electrons impact a convertor foil and the characteristic X radiation is produced. In the process, the convertor foil is vaporized into a cloud of highly energetic atoms. Specimens being exposed to the bremsstrahlung radiation must be protected from this debris. In addition, the conversion process has been shown to be optimized in terms of photon fluence for a heavy metal foil by using thicknesses three tenths of the mean electron range.[2] However, a majority of the electrons are not captured by such a thin foil and the specimens and calorimeters must also be protected from shine-through of these residual electrons. To perform these functions, the conventional convertor consists of three main components[3,4,5]: 1) conversion foil, 2) electron scavenger and 3) impulse shield or debris stopper. These components are held in a planar geometry by a retaining plate as shown schematically in Figure 1. Because the performance of the convertor is integrally coupled to the retaining plate, the plate may be considered a forth convertor component.

The efficient conversion of electron energy to photon energy requires a high atomic number (Z) target such as tantalum or tungsten.[4] The electron scavenger must be a low Z material to transmit the bremsstrahlung and absorb residual electrons. The electron scavenger must

also transfer the applied forces to the impulse shield--the structural member of the convertor. The applied forces result from the recoil of the convertor foil atoms during vaporization which dynamically loads the electron scavenger. A bulk graphite material is typically used for the electron scavenger,[4] although boron carbide[6] and water[7] have also been used successfully.

The impulse shield must also have good x-ray transmission properties and be sufficiently strong and stiff to withstand the blowoff forces without deflecting into the specimen and calorimeters. Limiting dynamic deflections to a minimum is an important consideration in convertor design. A minimum target-sample distance is required to obtain maximum dose in the sample because the produced photons diverge approximately as the inverse of axial distance.[4] Convertor design and materials selection are then governed by minimizing dynamic deflections with high specific strength and stiffness materials.

The low Z requirement severely restricts the use of common structural metals in the shield; however, aluminum and magnesium have been used at low fluences.[6] Although the properties of beryllium are attractive, it is not used for reasons of cost and toxicity. High performance filament-reinforced resin-matrix composites are the only other available low Z materials with sufficient strength and stiffness. An E-glass/polyester composite had proven to be the most successful impulse shield in previous work[4,6] for beam energies of 15-20 kilojoules. There are a number of reinforcements with a lower Z than glass which may be incorporated into a high performance convertor impulse shield; however, selection of an

advanced composite material for a given application involves the interaction of many composite variables (reinforcement, matrix, reinforcement form and orientation) with the operational environment. For example, although most of the properties of boron and carbon or graphite filaments are attractive for a convertor application, their limited impact resistance should eliminate them as candidate materials. Kevlar polyaramid filament (DuPont de Nemours and Co.), however, combines the impact resistance of glass[8] with higher stiffness and one-half the average Z of glass. As such, Kevlar is the most attractive replacement for glass as a convertor impulse shield reinforcement.

It is the purpose of this paper to present the results of a program conducted at the Rehyd test facility[9,10,11] to develop a bremsstrahlung convertor capable of surviving electron beam energies of 25-30 kilojoules. X-ray dose was monitored by deposition in Au foil calorimeters as described by Lockwood and Miller.[12]

Convertor Development

The first step in improving convertor performance was to identify the stress state in and the failure mode of the impulse shield. Initial evidence was conflicting, supporting both short time shock wave and longer time bending mode failures. Dolce,[4] using a 0.002 in. (0.05 mm) Ta foil, 0.125 in. (3.2 mm) ATJ graphite scavenger and 0.125 in. (3.2 mm) armor plate fiberglass impulse shield, noted specimens and calorimeters placed 0.5 in. (12.7 mm) from the impulse shield were impacted by the shield. Such large deformations are indicative of a bending stress state. Substitution of an armor plate Kevlar 49 (fabric style 1033)/polyester

composite for the impulse shield in the convertor arrangement used by Dolce[4] resulted in a larger permanent deformation of the impulse shield at a comparable energy level. This type of permanent deformation is seen in Figure 2 and is indicative of the internal damage sustained by the composite. The Kevlar 49-reinforced impulse shield theoretically should have shown less deformation due to its higher stiffness. This anomaly was caused by the high compliance of the 0.25 in. (6.35 mm) polycarbonate retaining plate. The large deformations were due to bending in the retaining plate with the impulse shield carried along. The stiffer Kevlar 49/polyester composite, which could not deform as easily as the retaining plate, picked up additional load and subsequently displayed larger permanent deformations than the fiberglass impulse shields.

Bending displacement in a plate may be estimated by Equation (1):[13]

$$w_{max} = \frac{k\, p_o\, R^4}{Et^3} \tag{1}$$

where

w_{max} = deflection

k = geometric factor

p_o = uniform load

R = plate radius

E = Young's modulus

t = plate thickness.

For the convertor retaining plate, the only quantities in Equation (1) which may be varied are E and t. A thicker plate is thus more effective in reducing deflection than is the substitution of a stiffer material. A combination of these effects was used in this program as a 3.0 in.

(76.2 mm) thick aluminum plate was substituted for the thin polycarbonate retaining plate. The convertor arrangement used throughout the balance of this discussion will consist of a 0.002 in. (0.05 mm) Ta foil, 0.125 in. (3.2 mm) ATJ graphite scavenger and a 0.170 in. (4.3 mm) composite impulse shield held in the thick Al retaining plate.

Once the high compliance of the retaining plate was taken out of the convertor system, the stress state in and controlling failure mechanism of the impulse shield could be determined. Identification of the failure mode was accomplished by substituting a graphite (Thornel 300)/epoxy composite for the ATJ graphite electron scavenger. The result is shown in Figure 3. The blown-out appearance of the graphite filaments toward the Ta foil could not be the result of structural bending. Such a result could only be caused by stress wave interactions. The extensive damage to the impulse shield shown in Figure 2 also points out the dispersion effect of the porosity in the ATJ graphite. The void-free Thornel 300/epoxy laminate transmitted the shock wave with little attenuation to the impulse shield which failed by spallation near the back surface. A similar result was obtained by substituting pressed B_4C for the ATJ graphite. In both cases, less damage would be expected had the principal loading been structural bending of the scavenger and shield unit. The porosity in the graphite electron scavenger appears to play a key role in convertor response. A short duration, large amplitude shock wave is attenuated as it travels through the porous graphite--a condition that reduces the possibility of failure in the impulse shield. The result for a B_4C scavenger is in conflict with the observations of

Oliphant[6] who attributed superior performance to the high ablation energy of boron carbide. It is possible that the B_4C used in his experiments contained a porosity distribution similar to that in graphite and thus acted to attenuate the shock wave in a similar manner.

Once the failure mode in the convertor impulse shield was identified as a shock wave phenomena, two approaches could be taken to design convertors capable of withstanding increased impulse loads: 1) increased energy absorption by the materials and/or 2) reduction of the stress wave amplitude. A combination of these approaches should provide the optimum convertor configuration. Energy absorption can take place by the mechanism of delamination between plies in a composite laminate. For this to occur, the incoming compressive wave must be reflected at the back surface as a tensile wave. Delamination by spallation will occur when the magnitude of the tensile stress pulse exceeds the composite interfacial strength.

Porosity in the composite impulse shield also appears to be effective in attenuating the stress pulse. This effect is seen in the micrographs of three impulse shields (Figure 4), all tested in the same convertor configuration. The 1033 Kevlar fabric/polyester laminate in Figure 4a is an armor material specially fabricated for ballistic purposes (Russell Plastics Technology, Inc., Lindenhurst, N.Y.). As such, it contains up to 25 percent porosity. The Kevlar 181 (50 x 50 picks/inch, 380 denier, 8 harness satin) fabric/epoxy laminate shown in Figure 4b was fabricated to theoretical density. The dense composite does not

attenuate the stress wave as much as the porous composite (4a) and spalls close to the back surface in a catastrophic manner rather than by internal delaminations. The geometry of the fiber bundles and loose weave of the 1033 fabric may also have an attenuating effect.

The quasi-isotropic (0, 90, ±45) tape layup shown in Figure 4c also does not attenuate the stress wave like the 1033 cloth; however, the greater strength of this composite suppresses severe spallation near the back surface and ultimately absorbs a portion of the stress pulse through a spall induced delamination in the interior of the plate. Once delamination has occurred, the remaining ligament of the quasi-isotropic plate is stiff enough to prevent large deflections during the longer duration ring-down of the trapped pulse. This is not the case for the 1033 fabric, however. The loose weave allows large magnitude deflections in the remaining ligaments as seen in Figure 4a. The quasi-isotropic tape layup provides a maximum in strength and bending stiffness which results in minimum convertor deflection; however, once the tensile strength of the filaments is exceeded, catastrophic failure of the type shown in Figure 3 will result. Success then lies in reducing the stress pulse below the composite spall strength.

The impulse may first be modified at its source, the Ta foil. By introducing a standoff between the Ta and graphite, the vaporized atoms are allowed to expand prior to impinging upon the graphite. In the process, the atoms undergo multiple collisions, diverge and spread their energy out in time and over a larger area of the graphite. The resultant

effect on the impulse is most easily seen in the computer models of R. C. Reuter.[14] Using the WONDY[15] code, and a fixed electron deposition profile, Reuter examined the effect of Ta standoff distance on the maximum tensile stress in the composite impulse shield. While the absolute magnitudes of stress are not quantitative because of approximations in the materials equations of state, the trends shown should be correct.

The wave profiles for the case of no standoff are shown in Figure 5a. The major components of the waves are shown as they move toward the impulse shield with increasing time until shortly after reflection from the back face. In the calculation, neither the graphite nor the composite are allowed to fail. The maximum tensile stress under these conditions occurs in step 5 of the profiles shown. The attenuation in the graphite is seen in the comparison of steps 1 and 2. Wave profiles for the case of a 0.0625 in. (1.6 mm) standoff between the Ta and graphite are shown in Figure 5b. A dramatic change occurs in the shape of the stress pulse--the maximum compressive stress produced in the graphite is greatly reduced and is accompanied by a significant tensile tail. The maximum tensile stress occurs when the tensile tail combines constructively with the main pulse after it is reflected as a tensile pulse from the back surface of the impulse shield. This mechanism will promote internal spallation (delamination) in the composite while reducing the probability of catastrophic spallation of the back surface. The general result of Reuter's[14] study is that the magnitude of stress decreases hyperbolically with increasing standoff distance.

The stress pulse may be further modified by the introduction of an air gap between the graphite electron scavenger and composite impulse shield. Similar to the mechanism of stress reduction by a standoff, the internal gap is more effective because it is a longer time event. Briefly, the stress pulse reflects off the back surface of the graphite as a tensile wave and begins fracturing the graphite in tension. The stress waves then reflect back and forth in each graphite fragment as the fragment undergoes a rigid-body translation into the composite. During this process the shock waves are losing energy by interaction with rarefactions. In addition, impact of the fragments upon the composite is spread out in time, further attenuating the original pulse.

A schematic of the convertor configuration incorporating both Ta standoff and internal gap is shown in Figure 6. The benefits in reducing stress amplitude by these modifications may be seen in Figure 7, a micrograph of a 1033 Kevlar fabric/polyester impulse shield tested in the Figure 6 configuration. A comparison with the same material tested without standoff and internal gap at a slightly lower energy level (Figure 4a) reveals that composite internal damage has been spread over a larger area at a decreased severity. Permanent set in the impulse shield (Figure 7), an indication of dynamic deflection, has been reduced by a factor of 5 from the convertor shown in Figure 4a. In addition, the composite tested without standoff and gap shows evidence of the onset of back surface spallation, meaning that the impulse shield is being stressed to the strength limit of the fibers in that configuration. The only spall seen in Figure 7 is the numerous small internal delaminations, indicating that reduced stress levels are introduced into the composite in this convertor configuration.

A plot of impulse shield permanent set such as seen in Figure 2 versus dose to gold for this convertor is shown in Figure 8. The scatter in the test data is typical of this type of environment. Beam geometry, calorimeter diagnostics and variable porosity distributions in the composite impulse shield are the main sources of error leading to the extreme experimental scatter.

This type of data does provide useful trends, however, as seen in Figure 9 - a summary of experimental data demonstrating the effects of the design modifications previously discussed. Permanent deflection in the impulse shield is plotted versus x-ray dose at a normalized Ta to Au calorimeter distance. All impulse shields are of the 1033 Kevlar fabric/polyester type with the exception of the quasi-isotropic tape layup, a 0, 90, ± 45 degree laminate of 195 denier Kevlar yarn in an epoxy matrix. The straight line plots are least squares fits to a minimum of 20 experimental data points. The stress pulse attenuation effect of the standoff and internal gap is manifested in the increased slope and damage threshold (intercept) of the dose-damage curve. The higher strength and stiffness of the tape layup also results in improved performance. However, the tape layup is roughly 8 times as expensive as the 1033 cloth layup ($8.00/impulse shield) and should only be used for high energy level tests.

Future Work

Future efforts in convertor development will be directed towards optimizing the modifications discussed in this paper. Graphite porosity and thickness, standoff distance, and internal gap distance are all interrelated and should be optimized with respect to one another.

Multiple internal gaps, either through thin layers of graphite and/or composite, might provide considerably better performance and will be evaluated in high energy tests. Future composite materials development will include examination of reinforcement weave and three dimensional weaves. Materials such as Kevlar 29 filament (lower stiffness version of Kevlar 49) and tough thermoplastic matrices will be investigated.

Conclusions

The results of the convertor development program conducted at the Rehyd Electron Beam Test Facility allow us to make the following conclusions:

1. The retaining plate must have high bending stiffness to minimize convertor deflection.
2. Failure modes in the convertor impulse shield are due to shock waves. Design modifications must be aimed at stress pulse attenuation or increased resistance of the convertor materials to shock wave damage.
3. Porosity in convertor materials, standoff of convertor foil, and internal gaps between the electron scavenger and impulse shield are techniques shown to reduce stress wave amplitude.
4. Kevlar-reinforced resin composites provide the best combination of strength, stiffness and low atomic number for impulse shield materials.
5. Incorporation of these modifications is shown to substantially reduce damage in convertor impulse shields from that of conventional convertors.

Acknowledgments

The author would like to acknowledge the support of H. N. Woodall who conducted the E-beam experiments. The author would also like to thank P. B. Tollefsrud, W. R. Hoover and D. E. Munson for their many valuable suggestions and review of this manuscript.

References

1. H. Bethe and E. Salpeter, "Quantum Mechanics of One- and Two-Electron Systems," Encyclopedia of Physics, Vol. 35, 1957, Springer-Verlag, Berlin, pp. 88-436.

2. J. A. Halbleib, Sr., "Hydra Flash X-ray Program--Standard Convertor," Sandia Laboratories Report SLA-73-0501, Albuquerque, New Mexico, April 1973.

3. B. Ecker, Physics International Company Report PIFR-366/371, 1972.

4. S. R. Dolce, "Bremsstrahlung Production on Hydra," Sandia Laboratories Report SLA-74-0215, Albuquerque, New Mexico, July 1974.

5. J. A. Halbleib, Sr., "Theoretical Model for an Advanced Bremsstrahlung Convertor," J. Appl. Phy., 45, 9, September 1974, pp. 4103-4109.

6. W. F. Oliphant, "Development of Hardened Anodes for the Naval Research Laboratory Gamble Facilities," Proceedings of DNA Simulator Design Symposium, January 1971.

7. J. Hansen, "A 10 MeV Bremsstrahlung Convertor," Danish Atomic Energy Commission Research Establishment Risö Report Risö-M-1261, April 1971.

8. D. F. Adams and J. L. Perry, "Instrumented Charpy Impact Tests of Several Unidirectional Composite Materials," Fibre Sci. and Tech., 8, 1975, pp. 275-302.

9. T. H. Martin, "The Hydra Electron Beam Generator," IEEE Trans. on Nucl. Sci., NS-20, No. 3, 1973, p. 289.

10. D. L. Johnson, "REBA, A Pulsed Electron Beam Generator," Sandia Laboratories Report SC-DR-70-872, Albuquerque, New Mexico, Dec. 1970.

11. L. D. Posey, P. B. Tollefsrud, H. W. Woodall, D. H. McDaniel and R. E. Allred, "X-ray Simulation Development (U)," CRD Report, Proc. of Fifth Symposium on Nuclear Survivability of Propulsion and Ordnance Systems, Stanford Research Institute, Oct. 7-9, 1975.

12. G. J. Lockwood and G. H. Miller, "Response of Improved Hydra Calorimeters to Bremsstrahlung Deposition," Sandia Laboratories Report SAND75-0587, Albuquerque, New Mexico, December 1975.

13. J. P. Den Hartog, Advanced Strength of Materials, Chapter IV, McGraw Hill, New York, New York, 1952.

14. R. C. Reuter, Jr., "Selected Numerical Results for the Rehyd Convertor," Memo to R. E. Allred, Sandia Laboratories, Albuquerque, New Mexico, April 1975.

15. R. J. Lawrence and D. S. Mason, "WONDY IV - A Computer Program for One-dimensional Wave Propagation with Rezoning," Sandia Laboratories Report SC-RR-71-0284, Albuquerque, New Mexico, August 1971.

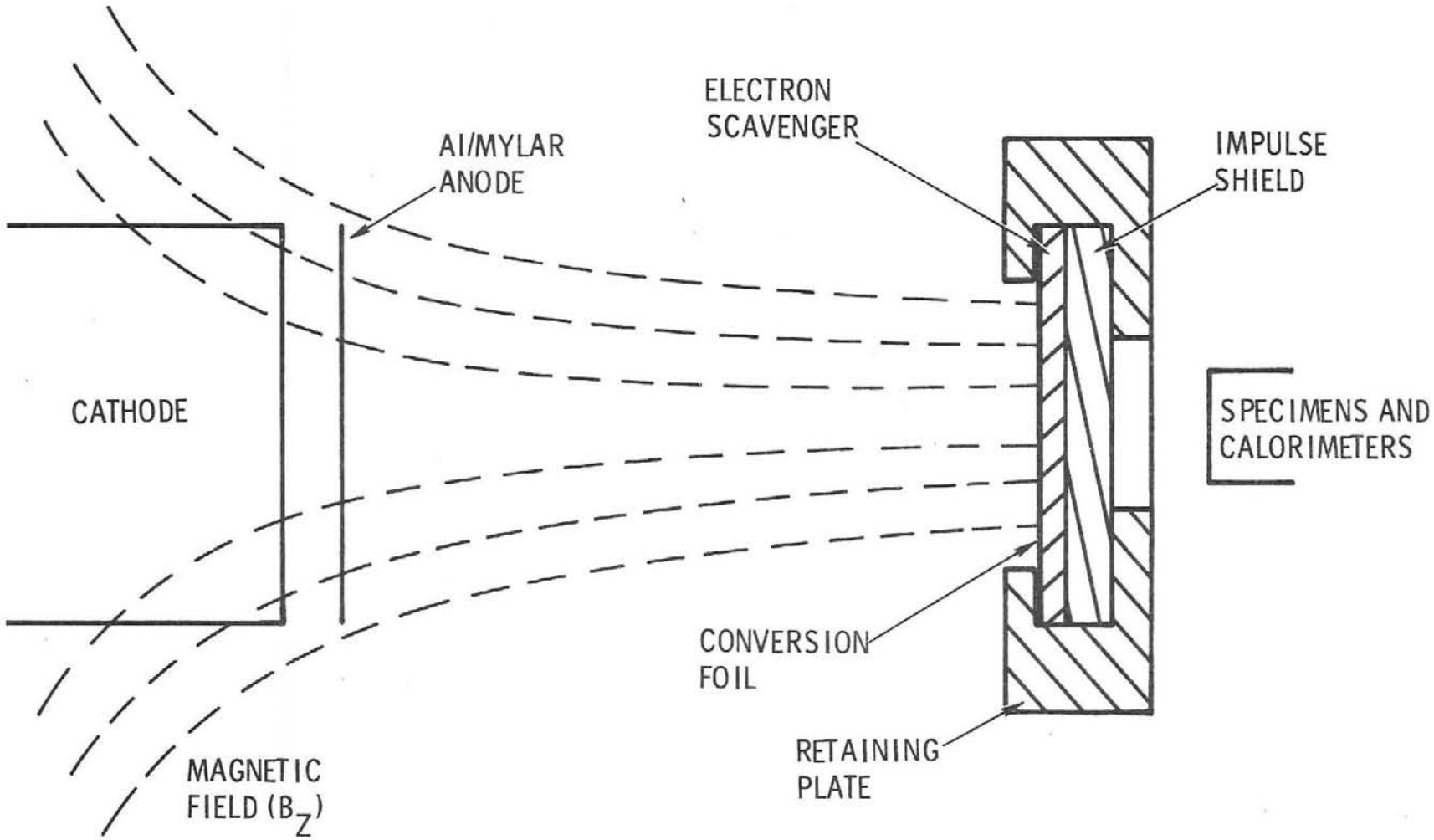

Figure 1. Conventional bremsstrahlung convertor configuration (schematic).

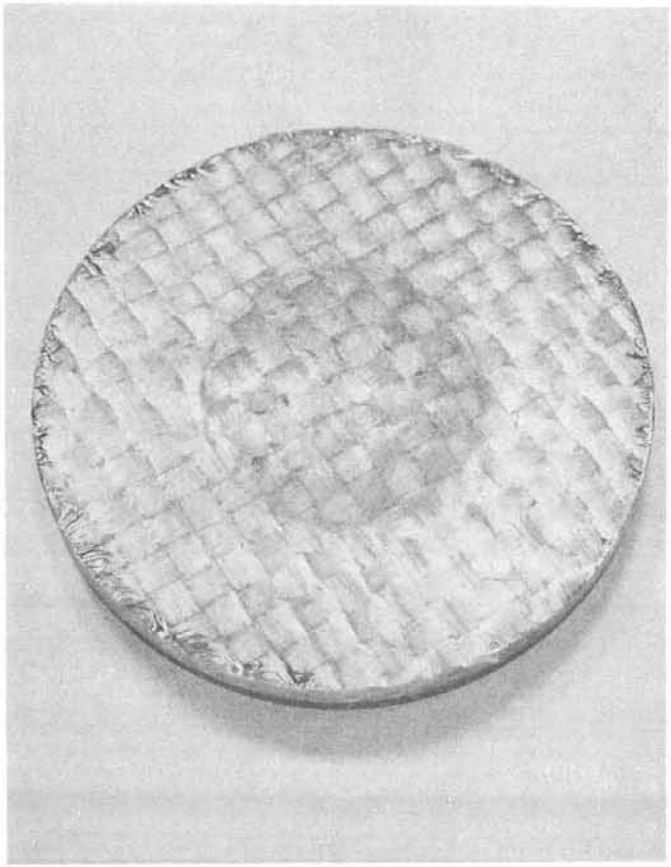

Figure 2. Deformation in exposed convertor impulse shield.

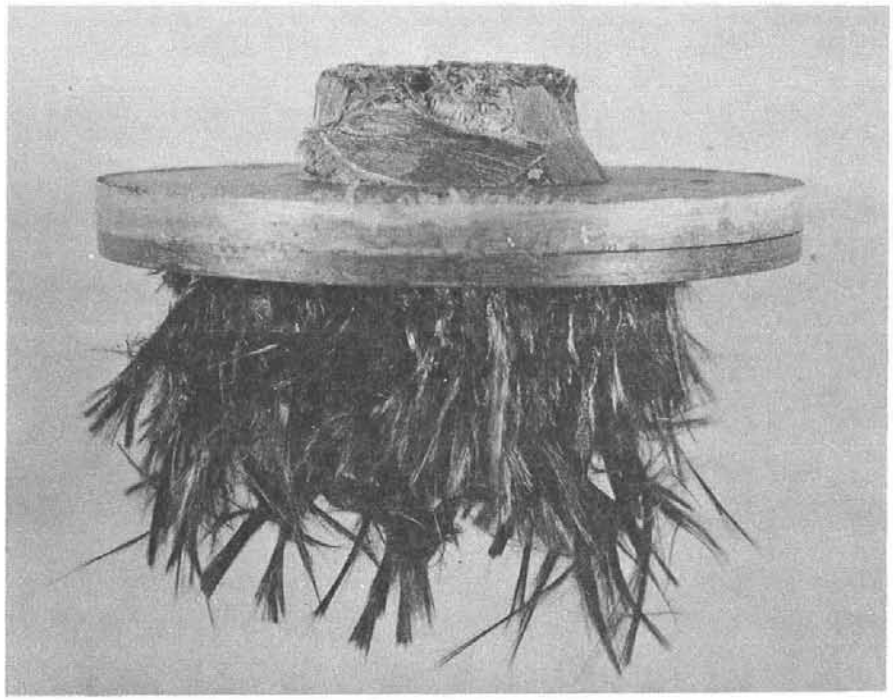

Figure 3. Catastrophic failure of convertor with a Thornel 300/ epoxy electron scavenger. Approximately 6.5 cal/gm Au.

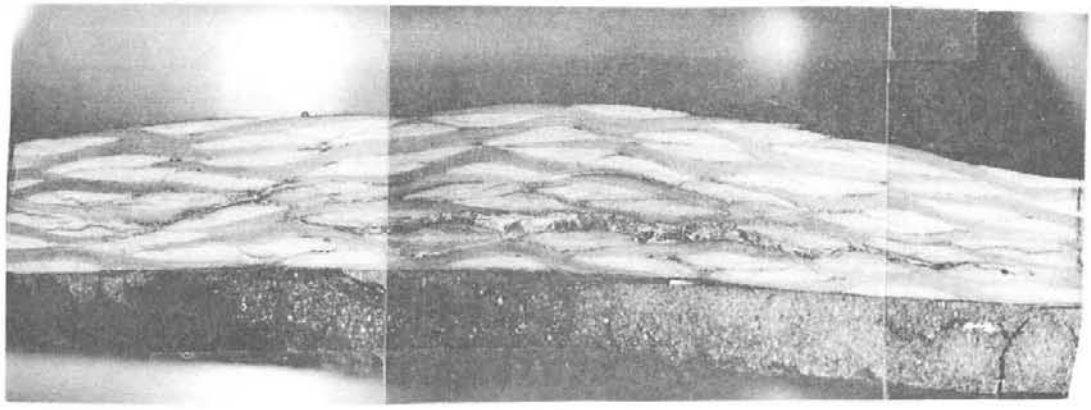

(a)

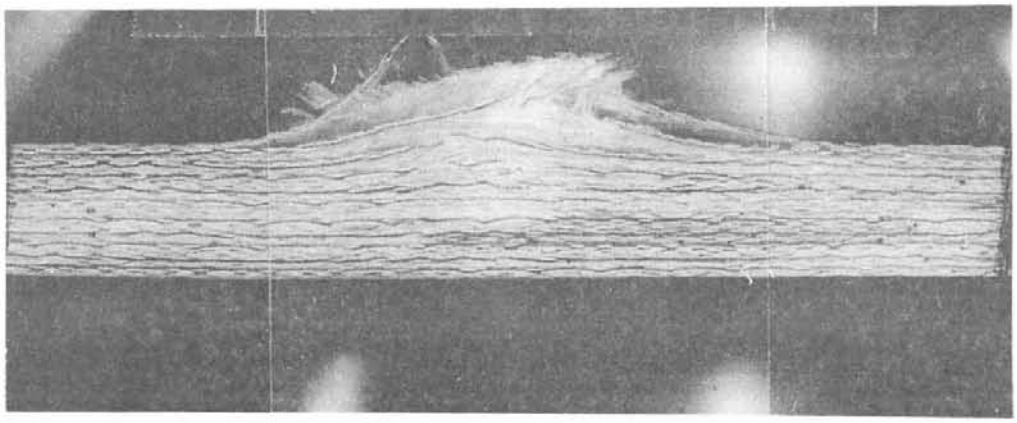

(b)

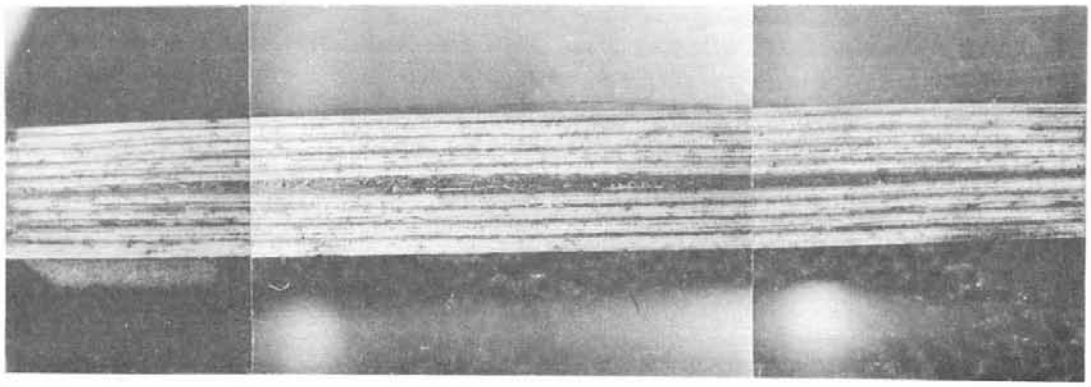

(c)

Figure 4. Micrographs of exposed Kevlar-reinforced impulse shields. (a) Style 1033 cloth, 7 cal/gm Au; (b) Style 181 cloth, 6.4 cal/gm Au; (c) 195 denier quasi-isotropic tape layup, 6.7 cal/gm Au.

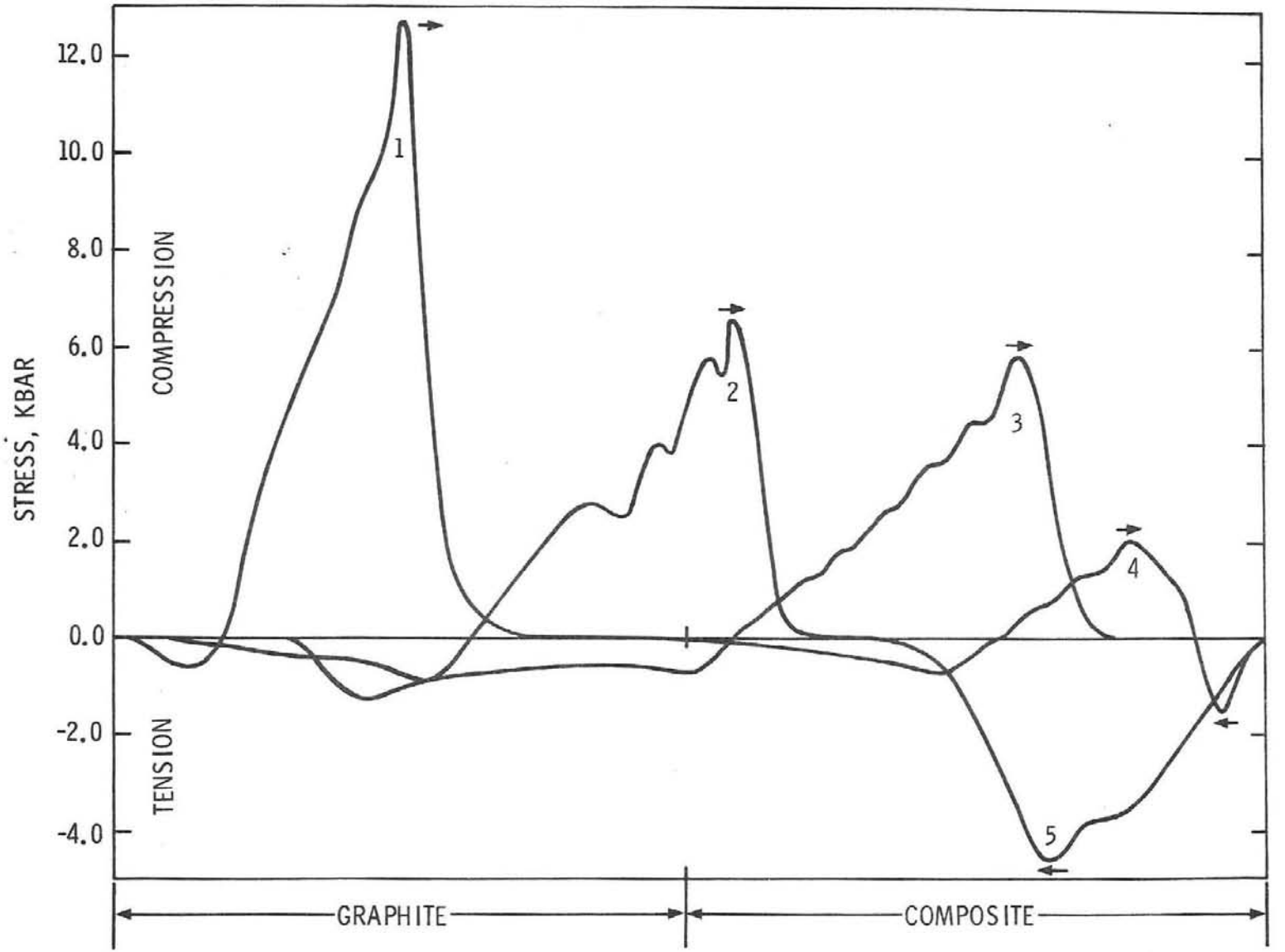

Figure 5a. Stress wave profile through convertor with no foil standoff.[14]

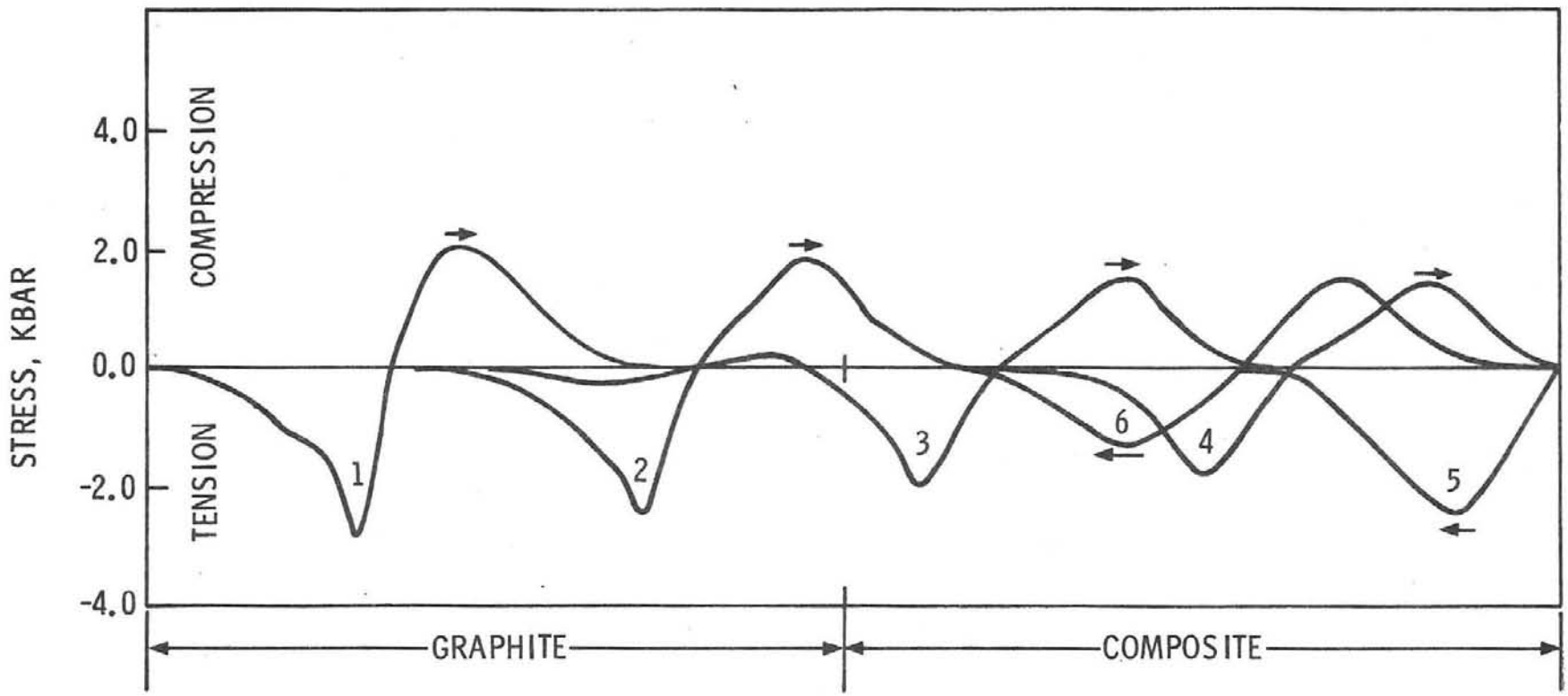

Figure 5b. Stress wave profile through convertor with 0.0625 in. (1.6 mm) Ta standoff.[14]

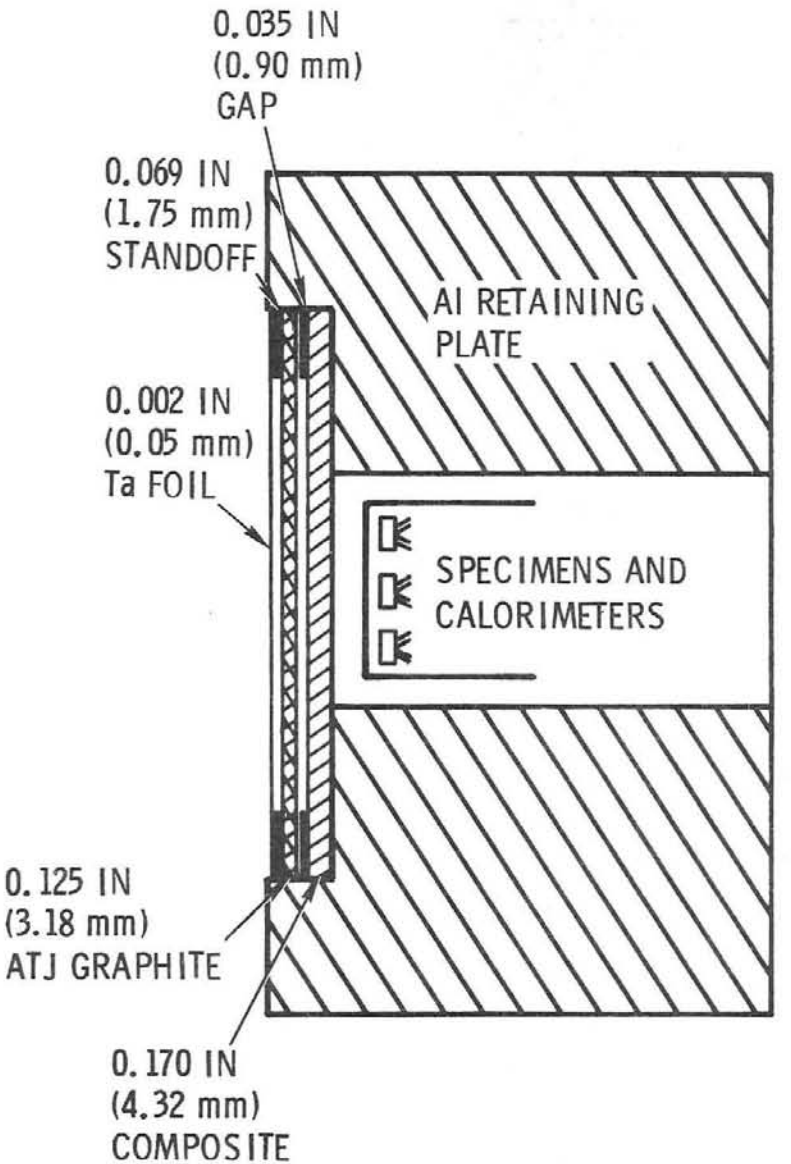

Figure 6. Schematic of improved convertor incorporating standoff, gap and thick retaining plate.

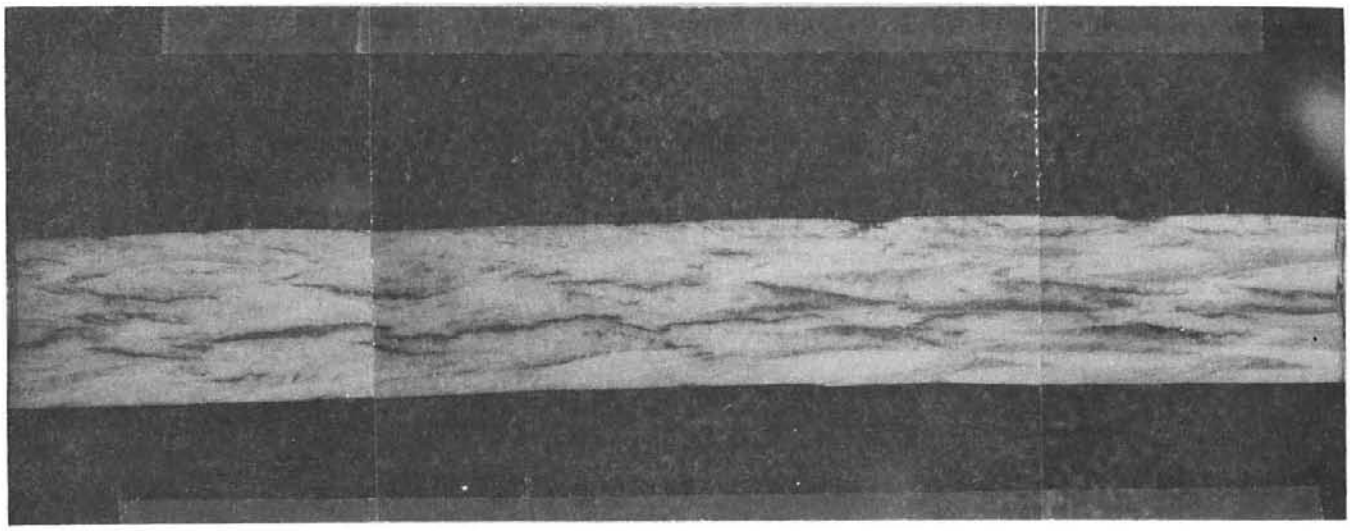

Figure 7. Style 1033 Kevlar fabric/polyester impulse shield tested at 7.6 cal/cm Au with standoff and internal gap.

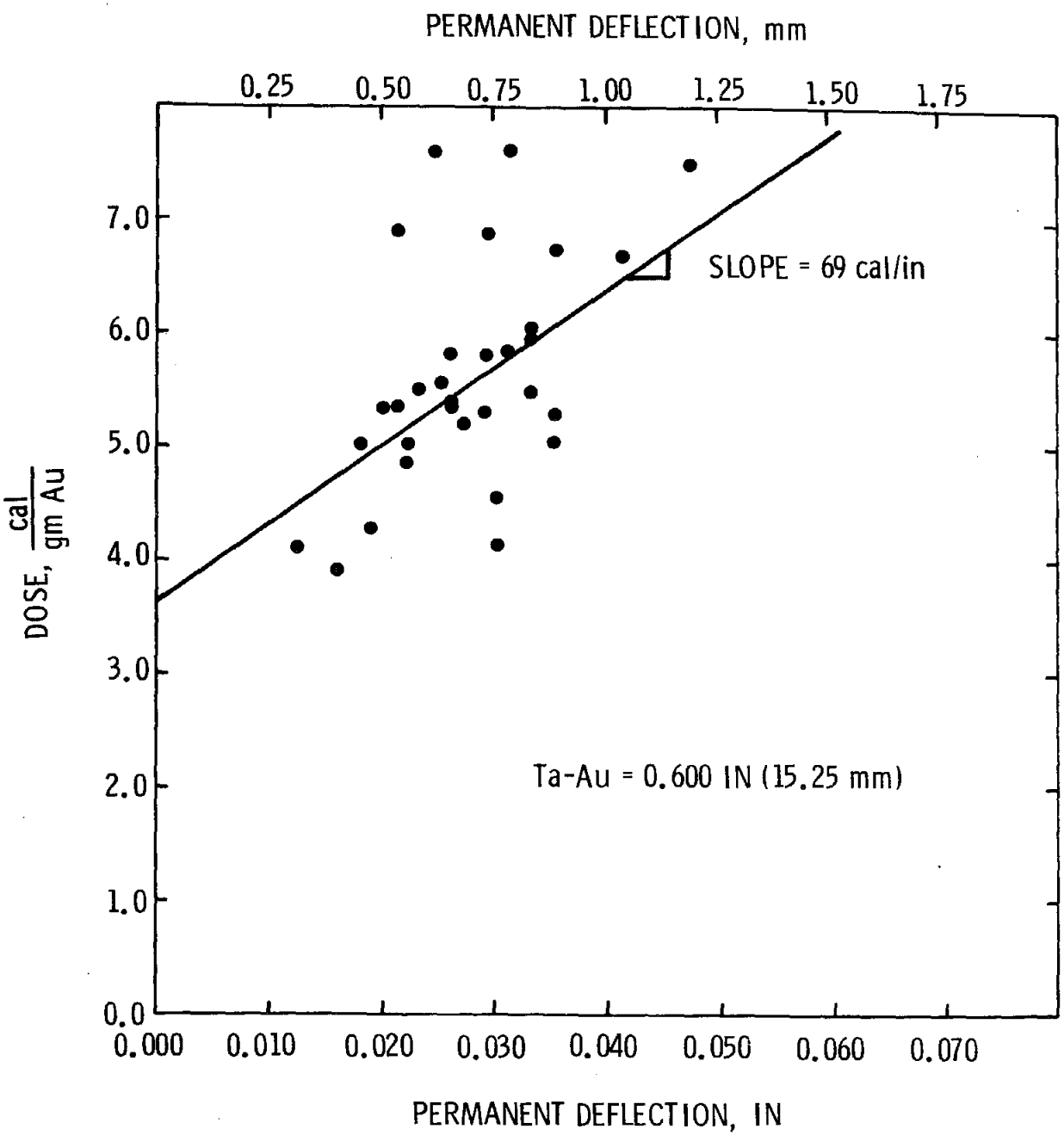

Figure 8. Response of improved convertor (Figure 6).

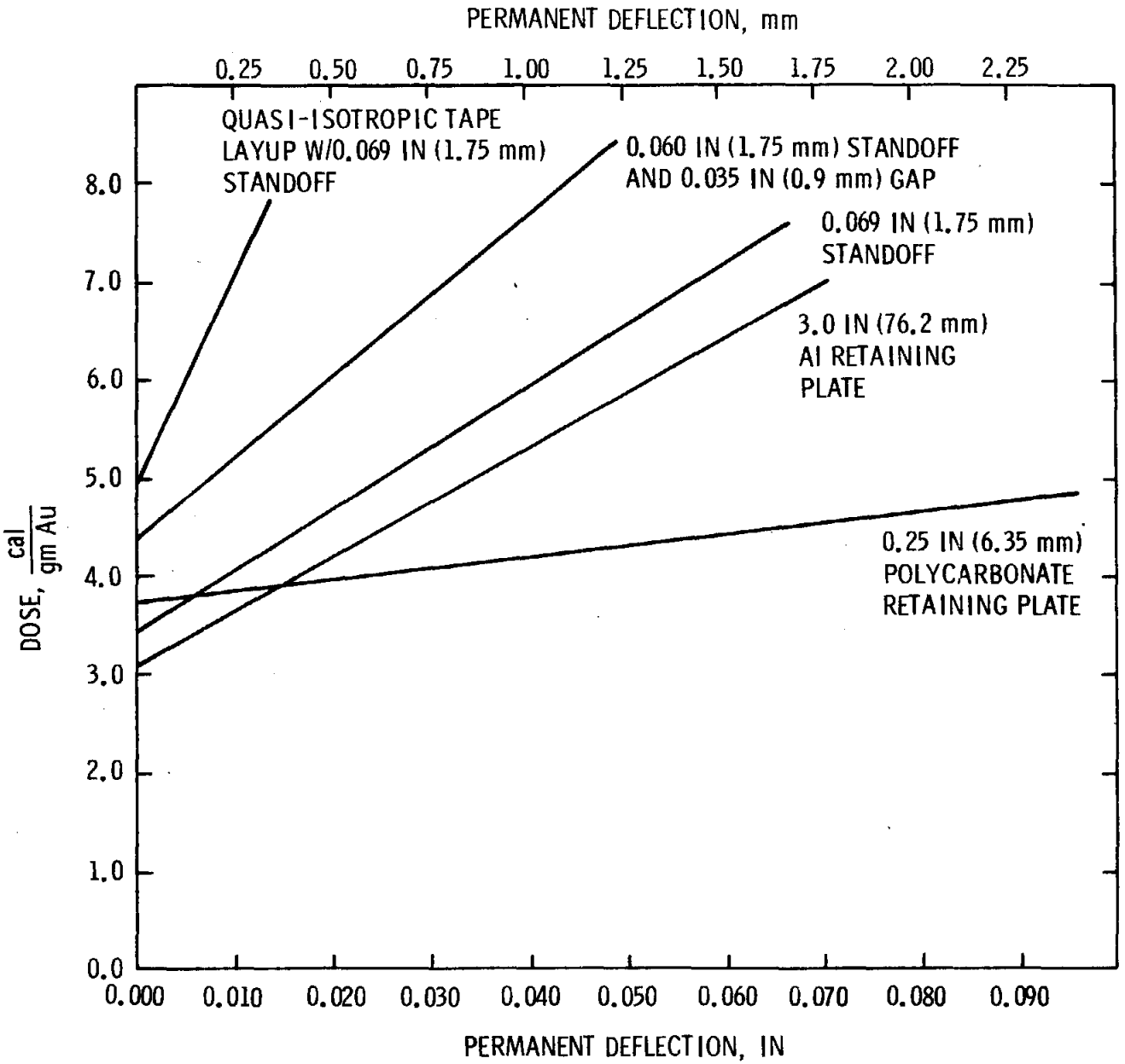

Figure 9. Impulse shield permanent deflection as a function of x-ray dose for various convertor geometries.

Distribution

F. W. Jones, UCC, Y-12 Plant
Attn: R. L. Huddleston (1)
C. E. Knight, Jr. (1)
L. Kovach (1)
T. T. Chiao, L-31, LLL
R. G. Dong, L-424, LLL
A. K. Thoeni - 862, BKC
R. H. Graham - 853, BKC
R. L. Sadler - 862, BKC

John Darrah (EL)
Kirtland AFB, NM 87117

Dr. P. Korn
Maxwell Laboratories, Inc.
Balboa Avenue
San Diego, CA 92123

Dr. S. Putman
Physics International Company
2700 Merced Street
San Leandro, CA 94577

Dr. R. A. Armistead
SRI
Menlo Park, CA 94025

Mr. P. Caldwell
Harry Diamond Laboratories
Branch 230
Washington, D.C. 20438

Mr. C. Jones
Pulsar Associates, Inc.
7911 Herschel Ave.
La Jolla, CA 92037

Dr. A. Wilson
Systems Science & Software, Inc.
P. O. Box 1620
La Jolla, CA 92037

Mr. R. Little
Simulation Physics, Inc.
41 B. Street
Burlington, MA 01803

Mr. Gerald Cooperstein
Naval Research Laboratory
Washington, D.C. 20375

1111 S. R. Dolce
1300 D. B. Shuster
Attn: 1320 M. L. Kramm
1330 R. C. Maydew
1340 T. B. Lane
1341 S. W. Key
Attn: J. T. Schamaun
1342 T. G. Priddy
1344 R. T. Othmer
Attn: P. P. Stirbis
1700 O. E. Jones
3600 L. M. Berry
Attn: 3620 R. S. Wilson
3622 T. P. Conlon
Attn: 3622-2 R. W. Weaver
3623 E. R. Frye
Attn: C. E. Albright, Jr.
F. H. Braaten
R. M. Rayner
4337 B. E. Bader
5000 A. Narath
Attn: 5100 J. K. Galt
5400 A. W. Snyder
5700 J. H. Scott
5131 P. L. Stanton
5160 W. Herrmann
5163 D. E. Munson
5167 B. M. Butcher
Attn: R. R. Boade
5200 E. H. Beckner
Attn: 5210 J. B. Gerardo
5230 M. Cowan
5240 G. Yonas
5260 K. J. Touryan
5230 P. B. Tollefsrud
5232 L. D. Posey
5232 H. N. Woodall
5233 M. J. Forrestal
Attn: R. I. Butler
5242 S. L. Shope
5712 R. C. Reuter, Jr.
5800 R. S. Claassen
Attn: 5810 R. G. Kepler
5820 R. L. Schwoebel
5830 M. J. Davis
5840 D. M. Schuster
5844 F. P. Gerstle, Jr. (2)
5844 R. E. Allred (10)
5844 B. L. Butler
5844 K. E. Mead
5847 T. R. Guess
8110 A. N. Blackwell
Attn: 8113 C. S. Hoyle
8114 W. D. Zinke
8150 D. E. Gregson
Attn: 8157 G. N. Beeler
8158 A. S. Rivenes

8310 R. H. Meinken
Attn: 8312 D. R. Adolphson
8314 H. J. Saxton
8360 J. F. Barham
Attn: 8362 G. R. Otey
9350 F. W. Neilson
Attn: 9351 D. W. Ballard
9352 O. J. Burchett
Attn: J. H. Gieske
9512-1 R. J. Martinez
3141 C. A. Pepmueller (5)
3151 W. L. Garner (3)
For ERDA/TIC (Unlimited Release)
3171-1 R. P. Campbell (25)
For ERDA/TIC
8266 E. A. Aas (2)